MEMORANDUM REPORT BRL-MR-3932

BRL

HEATING OF A TANK GUN BARREL: NUMERICAL STUDY

NATHAN GERBER
MARK L. BUNDY

AUGUST 1991

U.S. ARMY LABORATORY COMMAND

BALLISTIC RESEARCH LABORATORY
ABERDEEN PROVING GROUND, MARYLAND

NOTICES

Destroy this report when it is no longer needed. DO NOT return it to the originator.

Additional copies of this report may be obtained from the National Technical Information Service, U.S. Department of Commerce, 5285 Port Royal Road, Springfield, VA 22161.

The findings of this report are not to be construed as an official Department of the Army position, unless so designated by other authorized documents.

The use of trade names or manufacturers' names in this report does not constitute indorsement of any commercial product.

UNCLASSIFIED

REPORT DOCUMENTATION PAGE

Form Approved
OMB No. 0704-0188

1. AGENCY USE ONLY (Leave blank)	2. REPORT DATE	3. REPORT TYPE AND DATES COVERED
	August 1991	Final, Feb 90 - Feb 91

4. TITLE AND SUBTITLE
Heating of a Tank Gun Barrel: Numerical Study

5. FUNDING NUMBERS
PR: 1L162618AH80

6. AUTHOR(S)
Nathan Gerber and Mark L. Bundy

7. PERFORMING ORGANIZATION NAME(S) AND ADDRESS(ES)
U.S. Army Ballistic Research Laboratory
ATTN: SLCBR-LF-F
Aberdeen Proving Ground, MD 21005-5066

8. PERFORMING ORGANIZATION REPORT NUMBER

9. SPONSORING/MONITORING AGENCY NAME(S) AND ADDRESS(ES)
U.S. Army Ballistic Research Laboratory
ATTN: SLCBR-DD-T
Aberdeen Proving Ground, MD 21005-5066

10. SPONSORING/MONITORING AGENCY REPORT NUMBER
BRL-MR-3932

11. SUPPLEMENTARY NOTES

12a. DISTRIBUTION/AVAILABILITY STATEMENT
Approved for public release; distribution is unlimited

12b. DISTRIBUTION CODE

13. ABSTRACT *(Maximum 200 words)*

Heating of a gun barrel by repeated firing is modeled in a computer program that solves the one-dimensional (radial) unsteady heat conduction equation by a second-order finite-difference procedure. Coupling with interior ballistics is accomplished by employing as input data the bore temperature and heat transfer histories computed by interior ballistics codes. Limited comparisons of outputs with experimental results show favorable agreement (20% differences or less). The code is exercised to study a number of aspects of the heat transfer process qualitatively (e.g., time history of heat transfer before and after shot exit) and to relate the current model to a more simplified analytical-empirical model.

14. SUBJECT TERMS
barrel heating; multiple rounds; gun barrel heating mode; M256 120-mm gun; tank guns; gun barrels

15. NUMBER OF PAGES
41

16. PRICE CODE

17. SECURITY CLASSIFICATION OF REPORT	18. SECURITY CLASSIFICATION OF THIS PAGE	19. SECURITY CLASSIFICATION OF ABSTRACT	20. LIMITATION OF ABSTRACT
UNCLASSIFIED	UNCLASSIFIED	UNCLASSIFIED	UL

NSN 7540-01-280-5500

Standard Form 298 (Rev 2-89)
Prescribed by ANSI Std Z39-18
298-102

UNCLASSIFIED

INTENTIONALLY LEFT BLANK.

TABLE OF CONTENTS

INTENTIONALLY LEFT BLANK.

LIST OF FIGURES

INTENTIONALLY LEFT BLANK.

ACKNOWLEDGMENT

The authors gratefully acknowledge the help received from the following individuals: Mr. Paul Conroy, Ballistic Research Laboratory, Interior Ballistics Division, who supplied the input data files of T_g and h_g; Mr. Joseph Cox, Benet Laboratories, who supplied data upon which the authors based their specific heat; and Mr. James Bradley, Ballistic Research Laboratory, Launch and Flight Division, whose programming assistance was invaluable.

INTENTIONALLY LEFT BLANK.

1. INTRODUCTION

Continuous gun firing elevates the barrel temperature, producing several adverse effects on system performance. Accuracy, and hence lethality, is diminished with repeated firings due, in part, to thermal distortion of the barrel. Thermal signature, and hence vulnerability of the firing platform, also increases with firing rate and number of rounds fired. In addition, rapid firing of the gun increases the concern that the chamber wall temperature could cook off a subsequent round. Barrel wear also increases with gun tube temperature. To investigate the magnitude of these effects and seek ways of mitigating their detrimental effect on the overall gun system, the U.S. Army has embarked on a comprehensive thermal management program. Computer modeling is an integral part of this effort, as witnessed by its use in the numerous reports being published on these subjects (Artus and Hasenbein 1989; Bundy, to be published; Chandra and Fisher 1989a, 1989b; Rapp 1990; Talley 1989a, 1989b).

Numerical modeling is the most common approach. Each model, however, is developed with specific objectives in mind, which makes its application unique. For example, in the multiple-round cook-off studies of Chandra and Fisher (1989a, 1989b), emphasis is placed on accurately modeling the barrel wall temperature in the combustion chamber over the relatively short time of the combustion and blowdown cycle, with no attention given to the post-blowdown external cooling effects between rounds (which are, admittedly, small in the gun chamber region). Similarly, in the single-round barrel wear-type studies of Talley (1989a, 1989b), attention is focused on the bore surface temperature over the first half-second after firing. On the other hand, in the multiple-round, full-barrel, first-cut thermal surveys of Artus and Hasenbein (1989) and Rapp (1990), less detailed (time-averaged) propellant heat input is used, with some consideration given to external cooling (through the use of free and forced air convection assumptions). The multiple-round, full-barrel temperature model of Bundy (to be published) uses experimentally measured external cooling rates, but it is empirical in nature and thus limited to the range of operating conditions upon which it was developed.

We seek to establish a full-barrel temperature modeling capability for the M1A1, 120-mm M256 tank gun. The method of solution will be finite-difference based and similar to that of Chandra and Fisher (1989a, 1989b). External cooling rates will be based on experimental data obtained for this particular (field-configured) gun system (with thermal shroud, bore

evacuator, muzzle reference system collimator, and standard M1A1 recoil mount system). Eventually, we wish to modify the programming to simulate passive and active, internal and external barrel cooling effects, with the long range goal of developing a capability to investigate the feasibility of various gun barrel cooling devices.

We intend to develop this model incrementally, documenting it in a series of reports, beginning herewith. This report concerns barrel heating and cooling in one dimension (radial). Nevertheless, it will be possible to illustrate the importance of accurate round-to-round heat input data in successfully predicting the temperature-time history within the barrel.

The two problems of determining the flow in the bore and the heating in the barrel are coupled in that both involve the temperature at the inner wall of the barrel. In principle, an iterative procedure should be applied between the two problems; however, that is frequently not practical. We shall perform only the first approximation here, assuming that the flow problem "drives" the heating problem. In this case, the interior flow equations usually contain an approximation for convective heat loss to the barrel.

We shall be following the lead of previous investigators in assuming that heat conduction in the axial direction may be neglected relative to that in the radial direction (e.g., see Corner [1950], Engineering Design Handbook [1965], Heiney [1979]). Furthermore, if we ignore the effects of gravity on convective heating and cooling, then the problem is axisymmetric, and there is no azimuthal conduction in a transverse plane. Thus, we begin by treating only unsteady radial heat flow through the annular barrel. Figure 1a shows a longitudinal cross section of the barrel of an M256 120-mm gun (vertical scale expanded). We should expect that our model, at this stage, would be most applicable at locations away from the corners.

To keep the model tractable, we make some further approximations. We neglect any heat addition to the barrel produced by shock wave heating ahead of the projectile and by friction heating caused by the passage of the projectile. We also omit thermal expansion of the metal barrel.

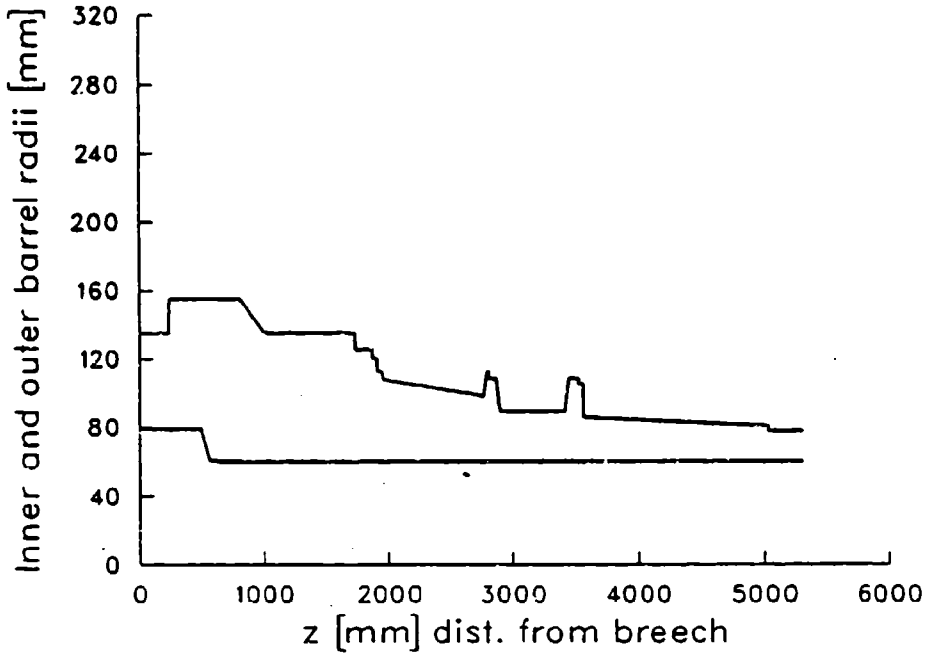

Figure 1a. Lengthwise Cross Section of M256 120-mm Gun Barrel (Stretched Vertical Scale).

Our approach, applicable to any gun barrel, is to calculate a numerical solution to the boundary-value problem that simulates the heat transfer processes. This calculation is carried out by the Crank-Nicholson implicit finite difference method (e.g., see Özisik [1968, 402]).

We shall perform computations, in particular, for a 120-mm M256 tank gun and compare results with experimental data. Additionally, we shall conduct a study relevant to the simplified model of Bundy (to be published), which provides a rapid approximate determination of the heating of the 120-mm M256 tank gun by repeated firing.

2. FORMULATION OF THE PROBLEM

We state our problem in terms of the following cylindrical coordinates: r, θ, and z.* The radial coordinate, r, is zero on the axis of the gun tube (z-axis) and varies from r_i to r_o, the concentric radii of the inner and outer walls of the barrel, respectively (Figure 1b). As stated in Section 1, the azimuthal angle, θ, does not enter the problem. The axial coordinate, z, is taken to be zero at the gun's breech. The barrel temperature, $T(r, z, t)$, where t is time

* Definitions of symbols are given in the List of Symbols section.

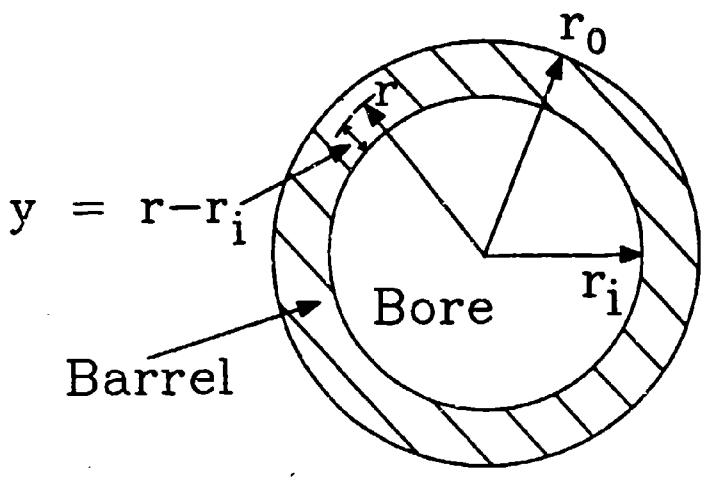

Figure 1b. Transverse Cross Section of Gun Barrel.

measured from the initiation of the first round, is determined by the following differential equation of heat conduction for a stationary, homogeneous, isotropic solid with no internal heat generation (Özisik 1968):

$$\rho c_p \, \partial T/\partial t = div\,[k\, grad\, T]. \tag{1}$$

Here the density, ρ, and the specific heat, c_p, of the metal are taken to be constant; * the quantity k is the thermal conductivity of the metal. With the simplifications of Section 1 and the further assumption that k is constant, Equation (1) becomes the Fourier Equation, namely,

$$\partial^2 T/\partial r^2 + (1/r)\, \partial T/\partial r = (1/\alpha)\, \partial T/\partial t, \tag{2}$$

where $\alpha = k/(\rho c_p)$ is the thermal diffusivity.

We now introduce the following notation: T_∞ = ambient temperature of the atmosphere, T_i = barrel temperature at the interior wall $r = r_i$, and T_o = barrel temperature at $r = r_o$. We assume an initially constant temperature, T_∞, everywhere. Thus, the initial condition at a given z is

* We note that c_p and k are actually functions of temperature; the effect of temperature dependence will be studied in a future investigation.

$$T(r,z,o) = T_\infty \qquad t = 0, \quad r_i \le r \le r_o. \tag{3}$$

The boundary conditions at the inner and outer walls are obtained by equating the rate of heat transfer from the surrounding gas at the wall to the rate at which heat flows from the wall into the barrel. The boundary condition at the inner wall is

$$k \;\; \partial T/\partial r - h_g \; T = -h_g \; T_g \qquad\qquad r = r_i, \; t > 0, \tag{4}$$

where $T_g\,(t\,,\,z)$ is the cross-sectional average temperature of the combustion products in the bore at time t and location z, and $h_g\,(t\,,\,z)$ is the coefficient of heat transfer between these products and the inner wall of the barrel (e.g., see Özisik [1968, 8–9]). In our model, T_g and h_g will be assumed known for any t and z and thus constitute input to the problem (see Section 3).

The boundary condition at the outer wall is

$$k \; \partial T/\partial r + h_\infty T = h_\infty T_\infty \qquad\qquad r = r_o, \; t > 0, \tag{5}$$

where the constant h_∞ is the coefficient of heat transfer between the barrel at $r = r_o$ and the surrounding atmosphere.

A computational difficulty arises at the start of the ballistic cycle due to the local temperature variation near the inner wall. This problem is circumvented by introducing a transformed variable ξ,

$$r = r\,(\xi) \qquad\qquad (0 \le \xi \le 1), \tag{6}$$

so that the constant increment $\Delta\,\xi$ will bunch the nodal points closely together near the inner wall but spread them out away from there.

We define our transformation in the following two steps:

$$\zeta = \gamma\xi + (1 - \gamma)\;\xi^\beta \qquad\qquad (o < \gamma \le 1, \; \beta > 2)$$

$$r = D\,\zeta + r_i, \tag{7}$$

where $D = r_o - r_i$, the barrel thickness, and γ and β are chosen constants. We have used $\gamma = 0.092$, $\beta = 2.25$. Note that $r = r_i$, r_o correspond to $\xi = 0,1$. Then Equation (2) transforms to

$$\partial T/\partial t = (\alpha/D^2)\,[f_1(\xi)\,\partial^2 T/\partial \xi^2 + f_2(\xi)\,\partial T/\partial \xi] \equiv G(\xi, t), \tag{8}$$

where

$$f_1(\xi) = \frac{1}{[\zeta'(\xi)]^2}$$

$$f_2(\xi) = \frac{D/\zeta'(\xi)}{D\,\zeta(\xi) + r_i} - \frac{\zeta''(\xi)}{[\zeta'(\xi)]^3}, \tag{9}$$

and where $(\,)' = d(\,)/d\xi$; the formulas for ζ' and ζ'' are given in Appendix A.

Equation (4) transforms to

$$k\,\partial T/\partial \xi - Dh_g\,\zeta'(\xi)\,T = -Dh_g\,\zeta'(\xi)\,T_g \qquad \xi = 0, t > 0, \tag{10}$$

and Equation (5) transforms to

$$k\,\partial T/\partial \xi + Dh_\infty \zeta'(\xi) T = Dh_\infty\,\zeta'(\xi) T_\infty \qquad \xi = 1, t > 0. \tag{11}$$

Then Equations (8), (10), (11), and (3) comprise the actual problem to be solved numerically. In the final printout, we revert to use of the independent variable, r, given by Equation (7).

In the present model, we assume that NR rounds are fired at the constant interval, t_f, between rounds. The input functions T_g and h_g are taken to be periodic, over period t_f, at all stations on the barrel. The subsequent barrel cooling after NR rounds can also be calculated.

3. INPUT DATA

3.1 Bore Temperature and Convective Heat Transfer. As stated previously, the temperature, T_g (t, z), and the convective heat transfer coefficient, h_g (t, z), of the gas in the gun bore are provided as input at the inner wall. The T_g and h_g values are obtained from calculations modeling the flow in-bore during a firing cycle. There are a number of models of the interior ballistics, with varying degrees of realism in simulation. Most of these compute "average" values for flow variable functions by ordinary differential equations. The NOVA code (Gough 1980), however, includes axial variation in the computation of the flow variables. It is the Veritay modification of this model (Chandra and Fisher 1989a, 1989b) that supplies T_g histories at eight chosen stations along the barrel. The values of h_g furnished by the Veritay code are obtained from the flow variables on the basis of the method of Stratford and Beavers (1961).

In the simplest simulation, one would model the in-bore flow for a single round out to about 1,000 s and would repeat as many times as needed only that portion of the history that covers the time interval $0 \leq t \leq t_f$. In practice, there are factors that complicate the flow model, such as loading a new round into the chamber. These factors will be neglected here.

A difficulty arises with use of the current NOVA model in that the numerical process stops operating at some time during the blowdown after the projectile exit from the muzzle. At present, the only means of extending the T_g and h_g curves is extrapolation. Each extrapolation curve will be required to have the same position and slope as the input curve at some time, t_B, and to approach asymptotically the ambient value of the variable as $t \rightarrow \infty$.

We employ an exponential extrapolation for $t \geq t_B$, where the break point, t_B, is taken to be 0.065 s. The time derivative, $\dot{T}$, is approximated at $t = t_B$ by a difference quotient $[T_g (t_B + \Delta t_g) - T_g (t_B - \Delta t_g)] / 2 \Delta t_g$, where Δt_g is the time increment in the T_g tables and $T_B = T_g (t_B)$.

$$T_g (t) - T_\infty = (T_B - T_\infty) \exp \left[\dot{T}_B (t - t_B)/(T_B - T_\infty) \right]. \qquad (12)$$

A similar formula is used for $h_g(t)$. Figures 2a and 2b show representative T_g and h_g histories at two stations on a 120-mm gun barrel. It is seen that T_g and h_g remain constant until the

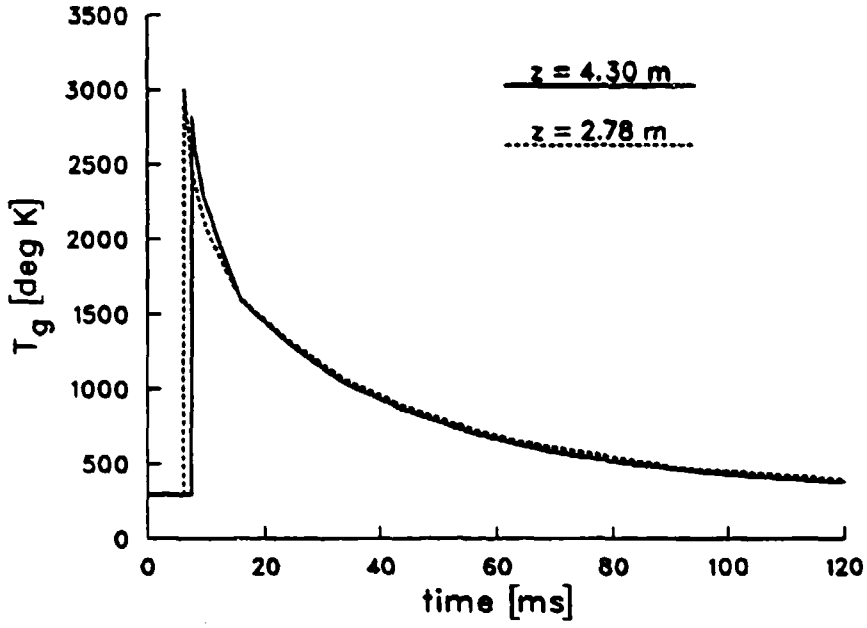

Figure 2a. Bore Gas Temperature Histories at Two Axial Locations.

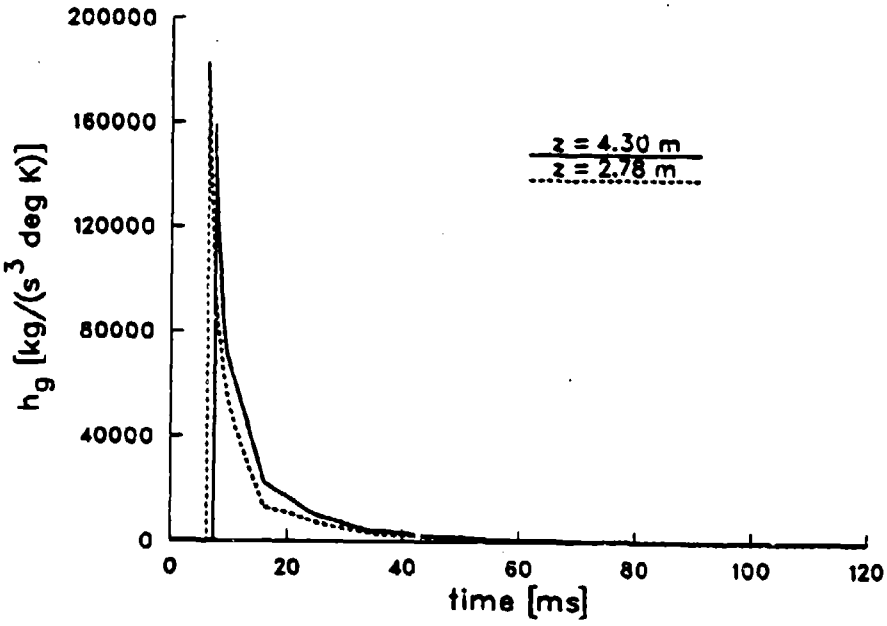

Figure 2b. Convective Heat Transfer Coefficient at Inner Wall of Gun Barrel at Two Axial Locations.

base of the projectile passes the given station at time $t = t_d$. At this time, these variables rise suddenly, then they decrease more gradually, with h_g decaying significantly faster than T_g.

3.2 Gun Properties and Ambient Conditions. All the computations reported here were performed for the case of an M256 120-mm tank gun firing a DM13 round. The dimensions of the gun barrel are shown in Table 1.

Table 1. Dimensions of M256 Gun Barrel

z (mm)	$2r_i$ (mm)	z (mm)	$2r_o$ (mm)	z (mm)	$2r_o$ (mm)
0.0	159.1	000.0	270.0	2,788.0	225.0
61.0	157.6	237.0	270.0	2,804.0	225.0
486.0	157.6	238.0	309.9	2,805.0	216.0
555.0	120.8	800.0	309.9	2,868.0	216.0
805.0	120.1	1,000.0	270.0	2,898.0	178.0
5,300.0	120.1	1,731.0	270.0	3,415.0	178.0
		1,732.0	250.0	3,445.0	216.0
		1,863.0	250.0	3,520.0	216.0
		1,864.0	240.0	3,521.0	210.0
		1,900.0	240.0	3,560.0	210.0
		1,901.0	225.0	3,561.0	171.0
		1,940.0	225.0	5,030.0	161.0
		1,950.0	215.0	5,031.0	155.0
		2,762.0	196.0	5,300.0	155.0

The values of properties of the gun barrel metal are taken to be

$$c_p = 469.05 \text{ J/(kg deg K)}^*$$

$$k = 38.07 \text{ J/(m s deg K)}$$

$$\rho = 7{,}827.0 \text{ kg/m}^3.$$

* The above value of C_p was measured by Joseph Cox, Benet Weapons Laboratory (1990), for M256 gun barrel steel at 295 K; the values for k and ρ were obtained from Talley (1989b) for 4335 steel; the value of h_∞ was obtained from experiments conducted by Bundy on a shrouded M256 barrel.

The ambient condition constants are

$$T_\infty = 294.8 \text{ K}$$
$$h_\infty = 12.0 \text{ J/(m}^2\text{s deg K)}.$$

4. FINITE-DIFFERENCE CALCULATION

In the Crank-Nicholson method employed here, all derivatives (except ξ derivatives at the walls) are approximated with central difference expressions. At the walls, ξ derivatives are obtained with three-point formulas. As a consequence, at each time step the temperature profile is determined by solving a set of $NI+1$ simultaneous linear equations, where NI is the number of intervals formed by the nodal (or grid) points between the inner and outer walls. The constant ξ increment is given by $\Delta\xi = 1/NI$. Figure 3 shows a diagram of the grid scheme for approximating Equation (8) at point P. The temperature is determined at time $t_{\ell+1}$ in terms of the temperature at the previous time step, $t_\ell = \ell\,\Delta t$, and the boundary condition at $t = t_{\ell+1}$, where Δt is the time increment.

We begin with the boundary conditions. At $\xi = 0$, Equation (10) is approximated by

$$[k/\{2D\,\Delta\xi\,\zeta'(0)\}]\,(3\,T_1^{\ell+1} - 4\,T_2^{\ell+1} + T_3^{\ell+1}) = h_g\,T_g - h_g\,T_1^{\ell+1}. \qquad (13)$$

Similarly, at $\xi = 1$, Equation (11) is approximated by

$$[k/\{2D\,\Delta\xi\,\zeta'(1)\}]\,(T_{NI-1}^{\ell+1} - 4T_{NI}^{\ell+1} + 3T_{NI+1}^{\ell+1}) = h_\infty\,T_\infty - h_\infty\,T_{NI+1}^{\ell+1}, \qquad (14)$$

where the subscript index denotes the nodal point, and the superscript index denotes the time.

For the interior points, $2 \le j \le NI$, the approximation of Equation (8) reduces to

$$T_j^{\ell+1} - (\Delta t/2)G_j^{\ell+1} = T_j^\ell + (\Delta t/2)\,G_j^\ell, \qquad (15)$$

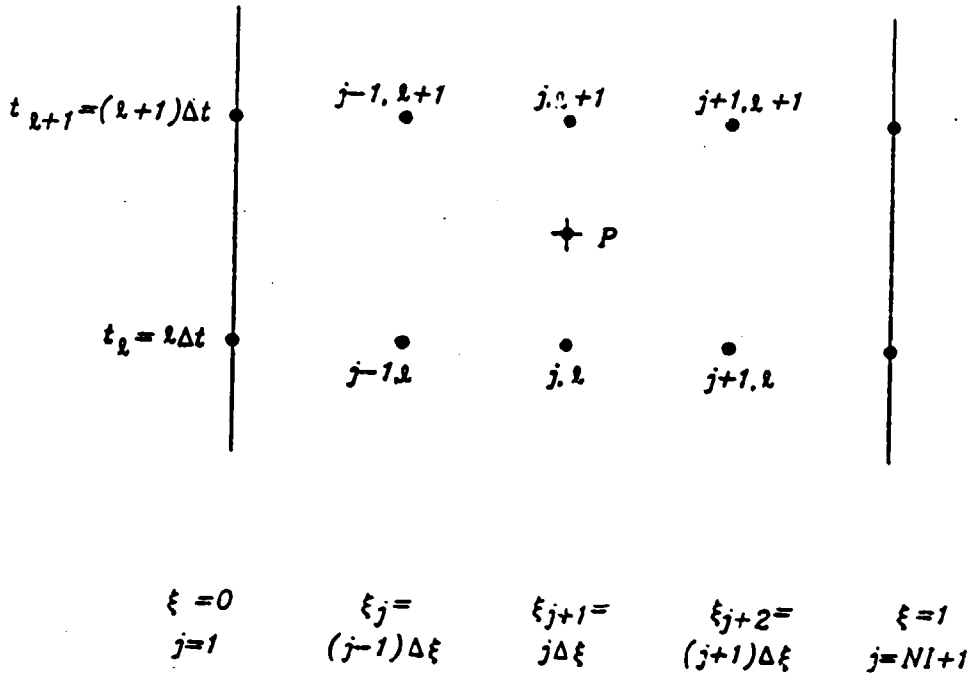

Figure 3. Grid Diagram for Numerical Solution.

where the right hand side is now known. The formula for G_j^ℓ (and $G_j^{\ell+1}$) contains $\partial T/\partial\xi$ and $\partial^2 T/\partial\xi^2$. These are approximated by

$$(\partial T/\partial\xi)_j \approx (T_{j+1} - T_{j-1})/(2\,\Delta\xi)$$

$$(\partial^2 T/\partial\,\xi^2)_j \approx (T_{j+1} + T_{j-1} - 2\,T_j)/(\Delta\xi)^2. \tag{16}$$

Then G_j for both $\ell\,\Delta t$ and $(\ell+1)\,\Delta t$ is given by the linear expression

$$G_j = g_1\,(\xi_j)\;T_{j-1} + g_2\,(\xi_j)\;T_j + g_3\,(\xi_j)\;T_{j+1}. \tag{17}$$

Formulas for g_1, g_2, and g_3 are given in Appendix A. Thus, Equations (13), (14), and (15) provide us with a set of linear equations for the temperature at $NI+1$ points at time $t = (\ell+1)\,\Delta t$:

$$\sum_{n=1}^{NI+1} A_{jn}\,T_n^{\ell+1} = d_j\,. \qquad (j = 1,\,2,\,\ldots\,NI+1). \tag{18}$$

The coefficients A_{jn} and d_j are given in Appendix A. A standard FORTRAN routine is applied to solve Equation (18); we have in most cases used $NI = 125$.

There is a problem in choosing Δt because there are essentially two time scales— (1) the duration of the firing (roughly 100 ms) and (2) t_f, the time between firings (usually 5 s or more when firing large guns). The Δt should be sufficiently small to resolve the phenomenon in case 1 but should be larger in case 2 to save time in computation. The program contains a subroutine prescribing Δt as a function of t within a firing cycle (see Appendix B).

The coefficients in the heat conduction equation (Equation 8) are assumed to be independent of t. Thus, only a single iteration is required to obtain the solution to the finite-difference equations. The Crank-Nicolson method is stable for all values of Δt, and there are no restrictions on the relative sizes of Δt and $\Delta\xi$.

5. ACCURACY CHECKS

At every time step, the following integral quantities are numerically evaluated:

$$Q_g\ (t) = 2\ \pi\ r_i \int_0^t h_g\ [T_g\ (\eta)\ -\ T\ (r_i,\eta)]\ d\eta \tag{19}$$

$$Q_\infty\ (t) = 2\ \pi\ r_o \int_0^t h_\infty\ [T_\infty\ -\ T\ (r_o,\eta)]\ d\eta \tag{20}$$

$$Q_b\ (t) = 2\ \pi\ \rho c_p \int_{r_i}^{r_o} r\ [T(r,t)\ -\ T_\infty]\ dr. \tag{21}$$

$Q_t = (Q_g + Q_\infty)$ is the quantity of heat per unit length of barrel that has entered the barrel through the inner and outer walls, and Q_b is the increase in the quantity of heat per unit length within the barrel since $t = 0$. A necessary, but not sufficient, condition for accuracy is that $Q_b = Q_t$. With the assumption of no errors in the code, poor agreement generally indicates that Δt and/or $\Delta\xi$ should be decreased. Empirical studies of temperature output vs. Δt and $\Delta\xi$ were additionally used as guides in choosing numerical parameters.

Figures 2a and 2b show that T_g and h_g experience sharp jumps at points along the bore just as the base of the projectile passes those locations. This produces a timewise discontinuity in the inner wall boundary condition. To study the "damage" that such a singularity might cause in our numerical output, we solve a simpler problem, both by our numerical scheme and by an approximate analytical method that is not affected by the singularity. The approximate method, which we designate the "thermal layer" method, is described in Chapter 7 of Özisik (1968). It is applicable only at very early times; an outline is provided in Appendix C. In this simpler problem, which differs from the main problem, the following conditions hold:

$$T = 0 \quad \text{for} \quad t \le 0, \quad r_i \le r \le r_o$$

$$T_g = T_{g\infty}, \quad h_g = h_{g\infty} \quad \text{for } t > 0, \tag{22}$$

where $T_{g\infty}$ and $h_{g\infty}$ are chosen constants; in addition, Equation (4) applies, and $T_\infty = 0$.

Figure 4 shows the temperature histories at the inner wall determined by the two methods for a given set of parameters. The good agreement between the two outputs is an indication that the finite difference method is not seriously affected by impulsive changes of variables in the bore.

6. COMPUTATIONAL RESULTS

6.1 Energy Considerations. The first topic of interest is the energy transferred from the bore to the gun barrel. Measurements (Talley 1989b; Brosseau et al. 1982) have been made of Q_A, the total heat transferred per unit area of the inner wall for a single round. The quantity Q_A is related to Q_b, computed here, by the relation $Q_A = Q_b/(2\pi r_i)$. Figure 5 shows computed values of Q_A at five locations on the barrel of an M256 120-mm gun that has fired a DM13 round. Also shown are experimental results* of Tally (1989b) and Brosseau et al. (1982). The largest discrepancy is roughly 19% at z = 5.18 m; reasonably good agreement is obtained for the other three comparisons.

Figure 6 provides, along with gas temperature and heat transfer coefficients, a representative history of heat delivery to the barrel for a single round. The location, z = 2.78 m, is approximately halfway along the length of the barrel. It is seen that at this location about 66% of the heat is transferred after the projectile has left the gun at t = 7.5 ms. Practically all the energy has been deposited by t = 40 ms even though the temperature of the gas in the bore is still decreasing significantly. Figure 6 indicates that the reason for this is the decay of the heat transfer coefficient (h_g) to a very small value by this time.

* The numbers of Talley and Brosseau were adjusted by multiplicative factors in order to match our use of c_p = 469.05 joules/(m^3 K) as the specific heat of the metal.

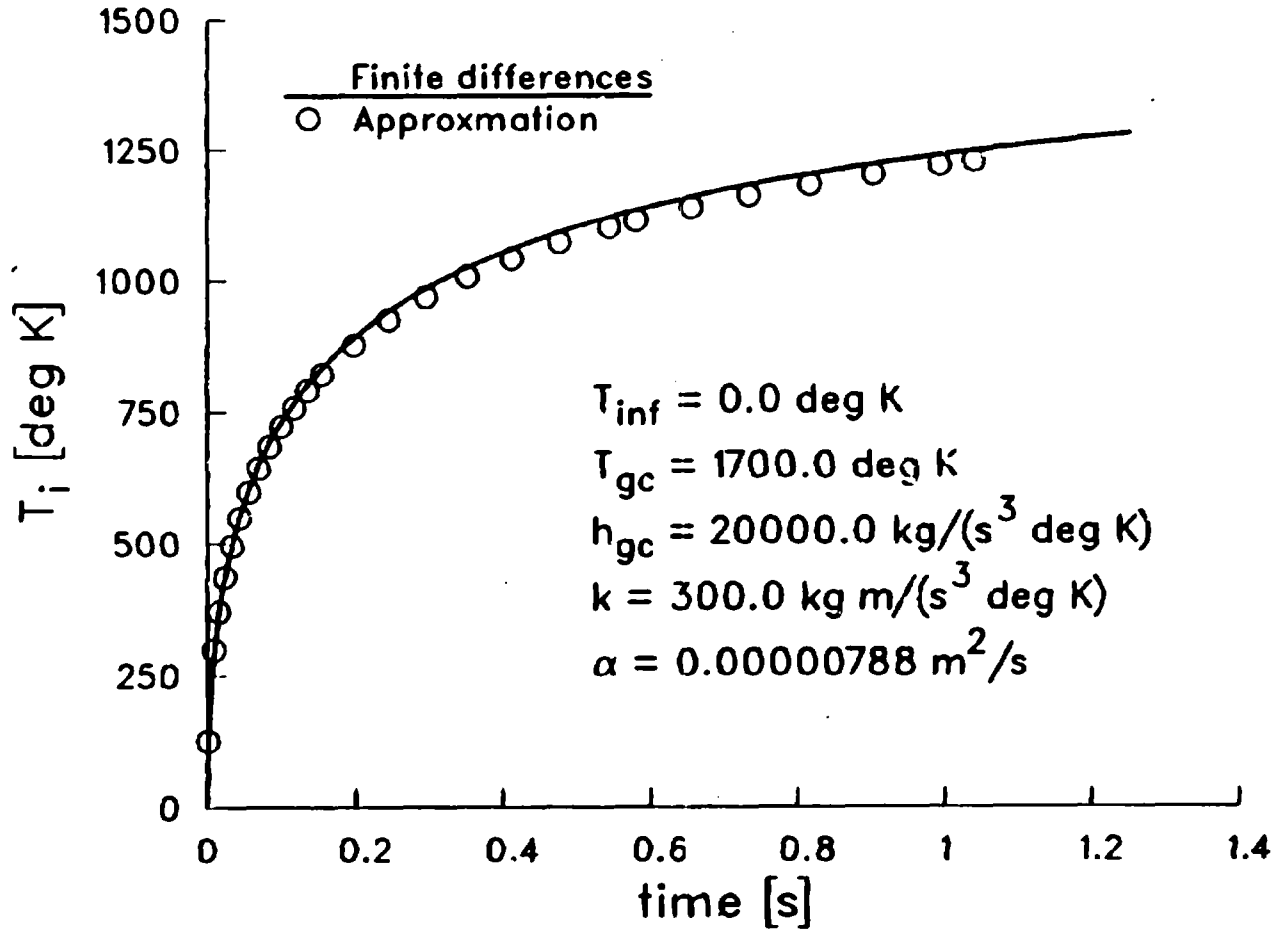

Figure 4. Inner Wall Temperature History for Test Problem: Numerical and Analytical Results.

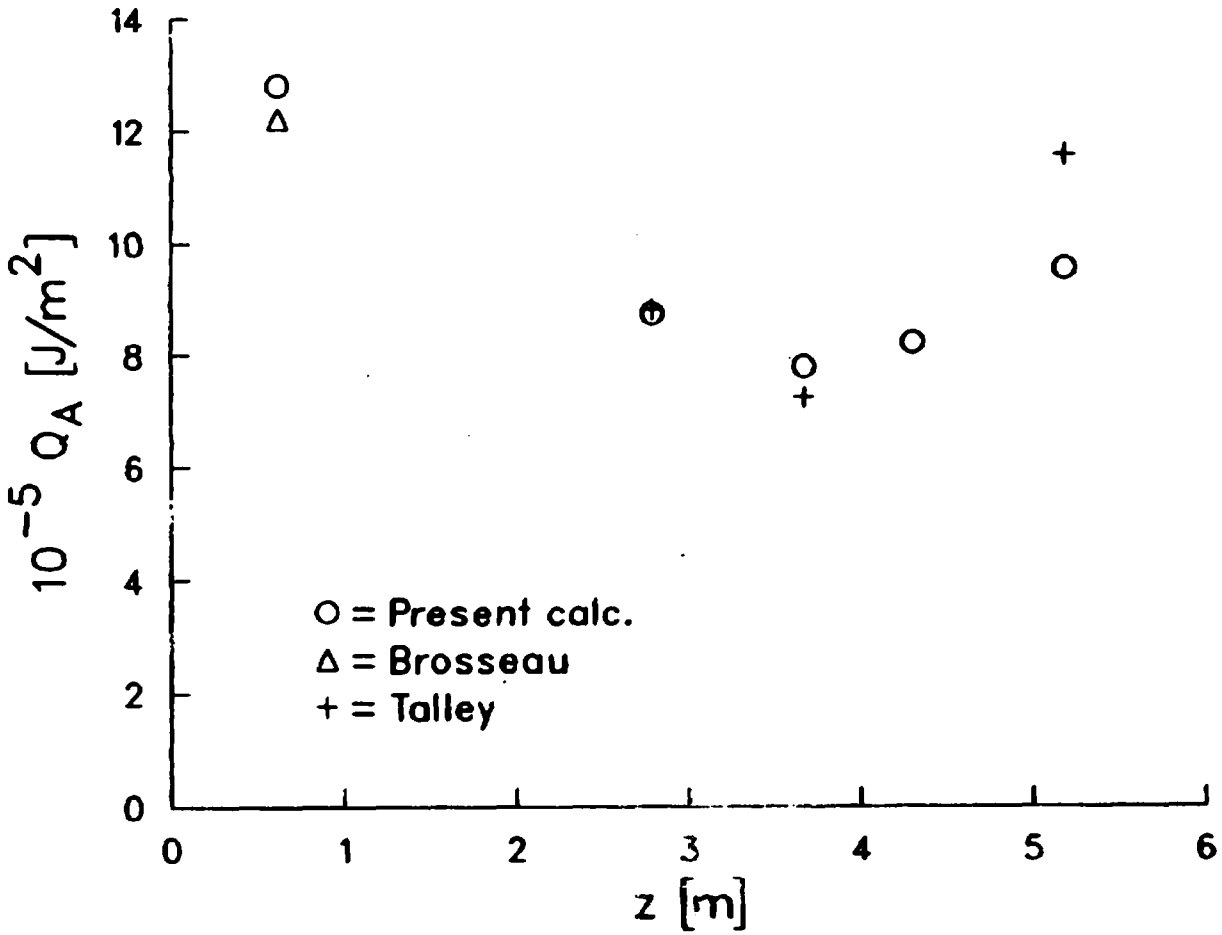

Figure 5. Heat Transferred to Gun Barrel in One Round: Numerical and Experimental Results.

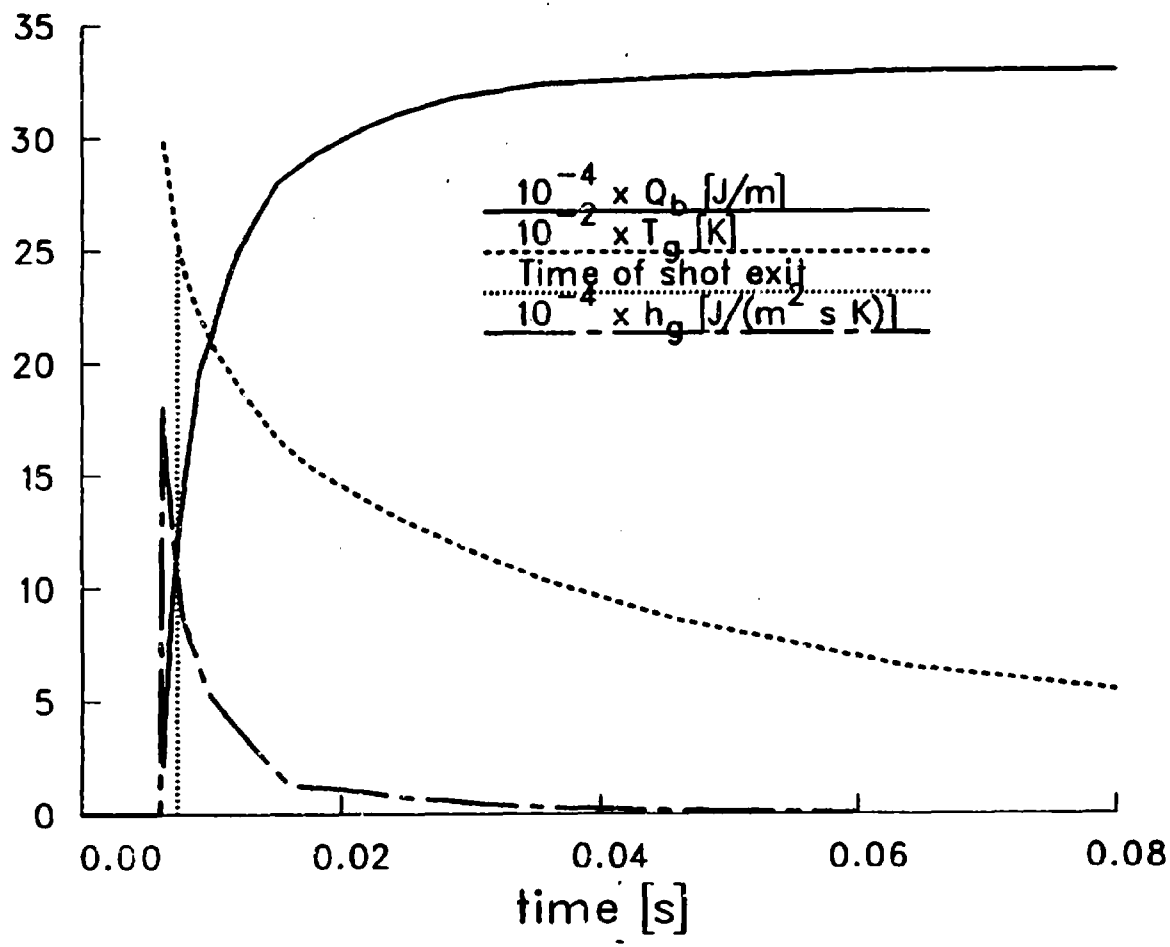

Figure 6. Heat Gain of Gun Barrel During Firing of Round at z = 2.78 m.

6.2 Speed of Heat Penetration. It takes a finite time after firing for a detectible temperature rise to be measured at a given point inside the barrel or on the outer wall. To obtain an estimate of the speed of heat penetration, we define the history of a "heat pulse" as the locus of the temperature $T = T_\infty + 0.5$ K in the r, t plane. (0.5 K is a change that can be measured by thermocouples.)

Figure 7 shows records of the heat pulses at three stations on the barrel. The three curves coincide for the durations of the z = 3.67 m and z = 5.18 m pulses. The times to reach the outer wall are approximately 19.5 s, 4.3 s, and 1.8 s at z = 2.78 m, 3.67 m and 5.18 m, respectively. For the most part, the velocity decreases with time. An exception occurs at z = 2.78 m (r_o = 0.11 m), where the pulse accelerates slightly after about 14 s. A test calculation with r_o = 0.16 m at z = 2.78 m produced a similar behavior, the acceleration beginning at about 72 s.

6.3 Outer Wall Temperature: Slow Rate-of-Fire. Figures 8a and 8b show the temperature histories for several radial stations at two axial locations computed for a slow rate of fire, namely, one round every 4 min. It is observed that for each round there is a time after firing when all the curves practically coalesce, implying the attainment of nearly constant temperature across the barrel. This time has been called the "soak-out time." It is also roughly equal to the "rise time," t_r, namely, the time (for a given round) when T_o attains its maximum. We shall henceforth just use the "rise time" expression. One cannot designate precisely a value for t_r, but one can estimate an approximate value from the curves. See, e.g., Figure 8a, first round. The rise time value seems to stay constant from round to round at a given station, but it changes with barrel thickness. Thus t_r = 100s at z = 2.78 m and = 14 s at z = 5.18 m.

The temperature behavior described above has been found to be fairly general. Henceforth, "slow" and "fast" rates-of-fire will refer to situations in which $t_r < t_f$ and $t_f < t_r$, respectively, where t_f is the interval between rounds.

Figure 9 presents a comparison between theoretical and experimentally determined (Bundy, to be published) values of rise of outer wall maximum temperature between successive rounds, 3 min apart, at z = 4.30 m. The two sets of points agree to within about 10%.

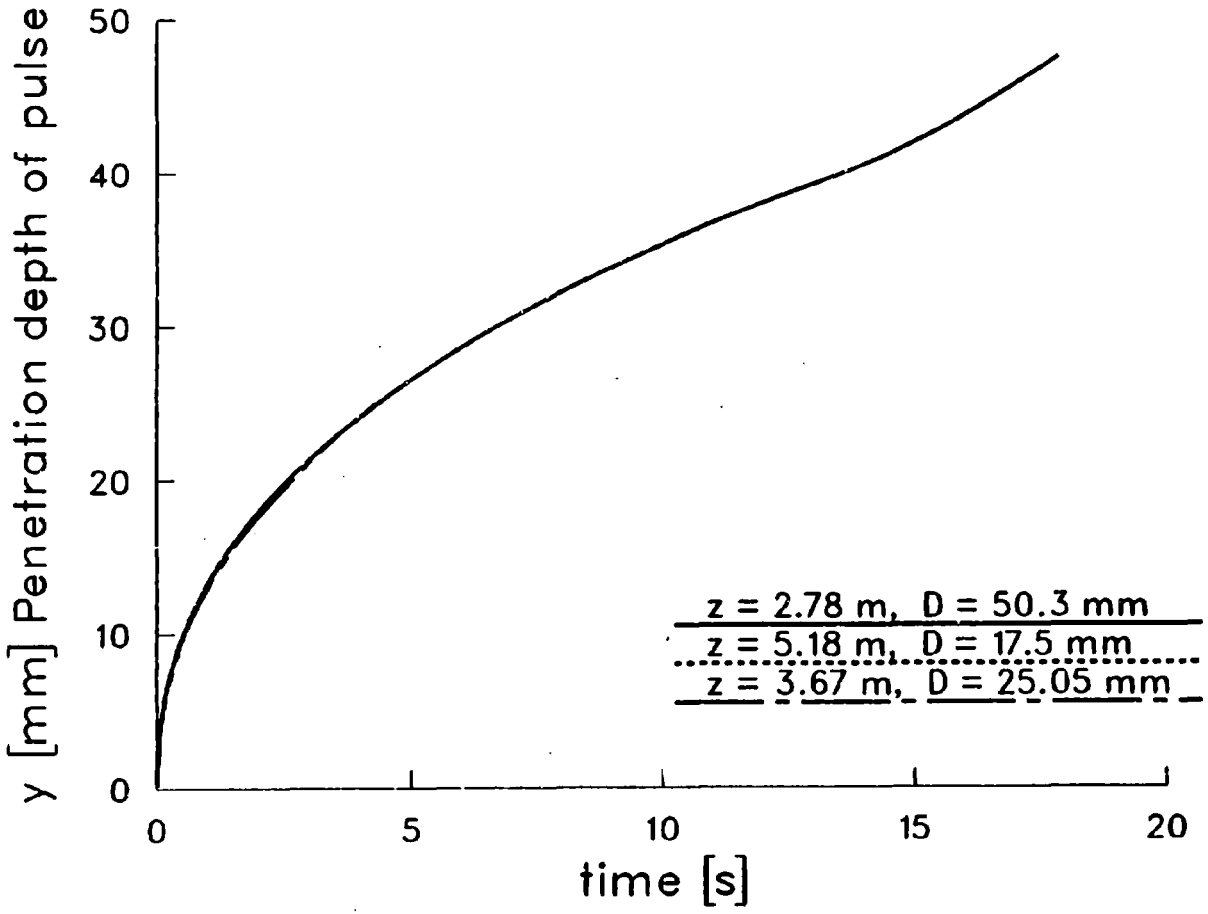

Figure 7. Histories of Radial Heat Pulse Travel at Three Axial Locations.

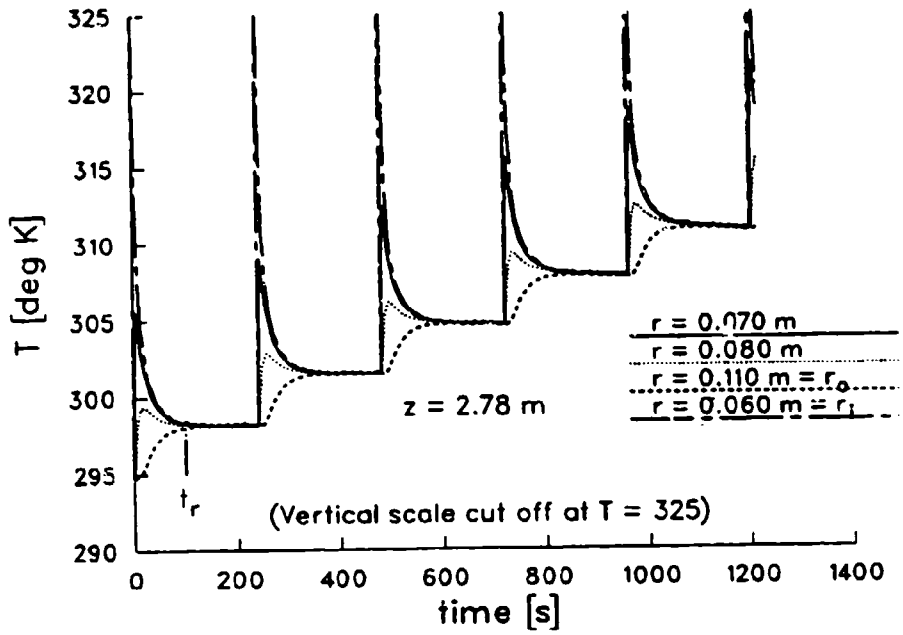

Figure 8a. Slow Rate-of-Fire (t_f = 4 min): Temperature Histories at z = 2.78 m.

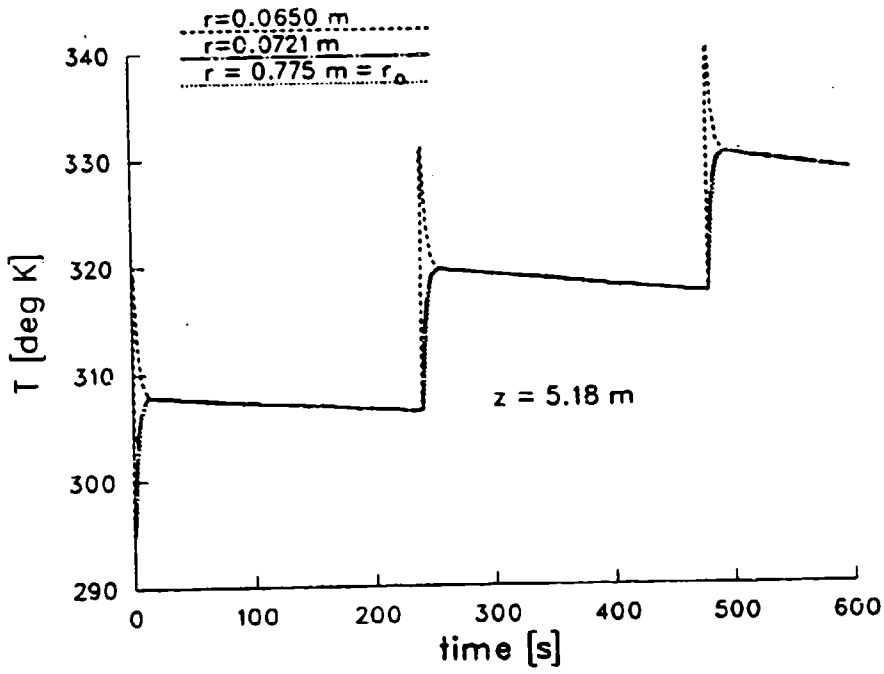

Figure 8b. Slow Rate-of-Fire (t_f = 4 min): Temperature Histories at z = 5.18 m.

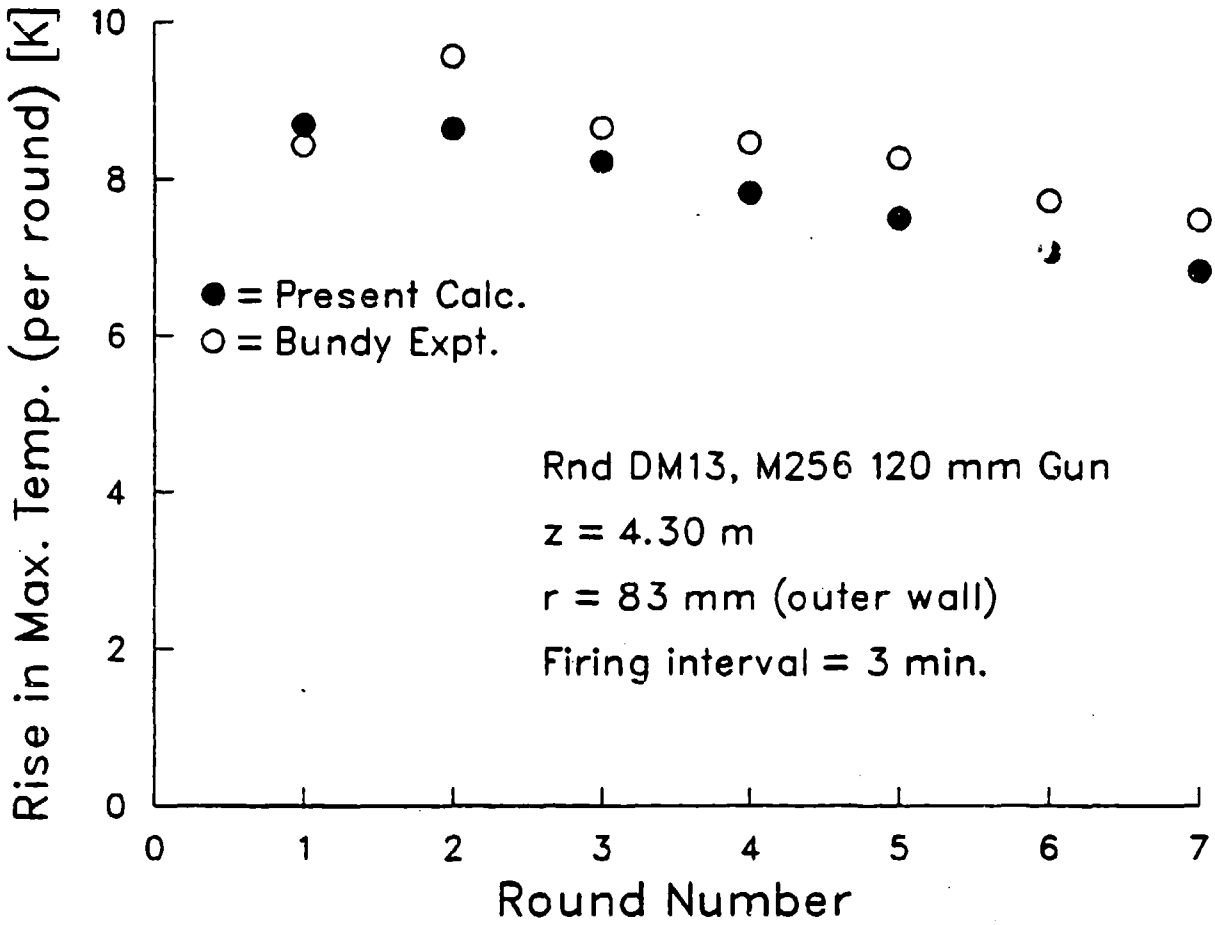

Figure 9. Rise in Maximum Outer Wall Temperature per Round: Numerical and Experimental Results.

6.4 Outer Wall Temperature: Fast Rate-of-Fire. Figure 10 shows the inner and outer wall temperature variations computed at z = 4.3 m (1 m from muzzle) for a 15-round burst of three rounds per minute. The increase in T_0 between the beginnings of the fifth and fifteenth rounds is 77.4 K. This number compares favorably with the corresponding experimental figure, approximately 75.7 K, read from the graph in Figure 13 of Bundy (to be published).

7. RELATION TO ANALYTICAL - EMPIRICAL MODEL

We examine some aspects of our simulation in relation to the simplified analytical model of Bundy (to be published) for gun tube heating. Mathematically, this model requires only the evaluation of formulas. It is also empirical, in that certain physical parameters employed are determined experimentally. Two advantages of this model are its low computational time on the computer and its ability to simulate a large variety of firing sequences. So far, only those parameter values that are applicable to an M256 120-mm gun firing DM13 rounds have been used. Figure 11 shows a typical example of results produced by this analysis.

For slow rate-of-fire, the model assumes that the outer wall temperature has a sawtooth-like variation with time, as in Figure 11. For each firing cycle, the left segment (always with positive slope) extends from the instant of fire through t_r, the rise time interval. The right segment, with uniform temperature across the barrel, extends to the next instant of fire. The rise times have been determined experimentally by temperature measurements on the outer wall of the barrel. It can be seen that this modeling is an idealization of the heating pattern depicted in Figure 8. In fact, rise times estimated from computations may be compared with measured values for checking purposes.

For fast rate-of-fire, the same sawtooth pattern cannot be used to simulate temperature time-variation. Figure 10, where $t_f / t_r = 0.72$, demonstrates this situation. Modeling will necessarily be more complex here. Details of the treatment of this case in the Bundy model are deferred to Bundy (to be published). One assumption, however, is that the heat input to the gun from each round will be complete before the next round is fired. This assumption is certainly valid for the conditions in Figure 6, which is a representative example of heat transfer history. The heat input time is about 40 ms, while times between rounds are at least of the order of several seconds.

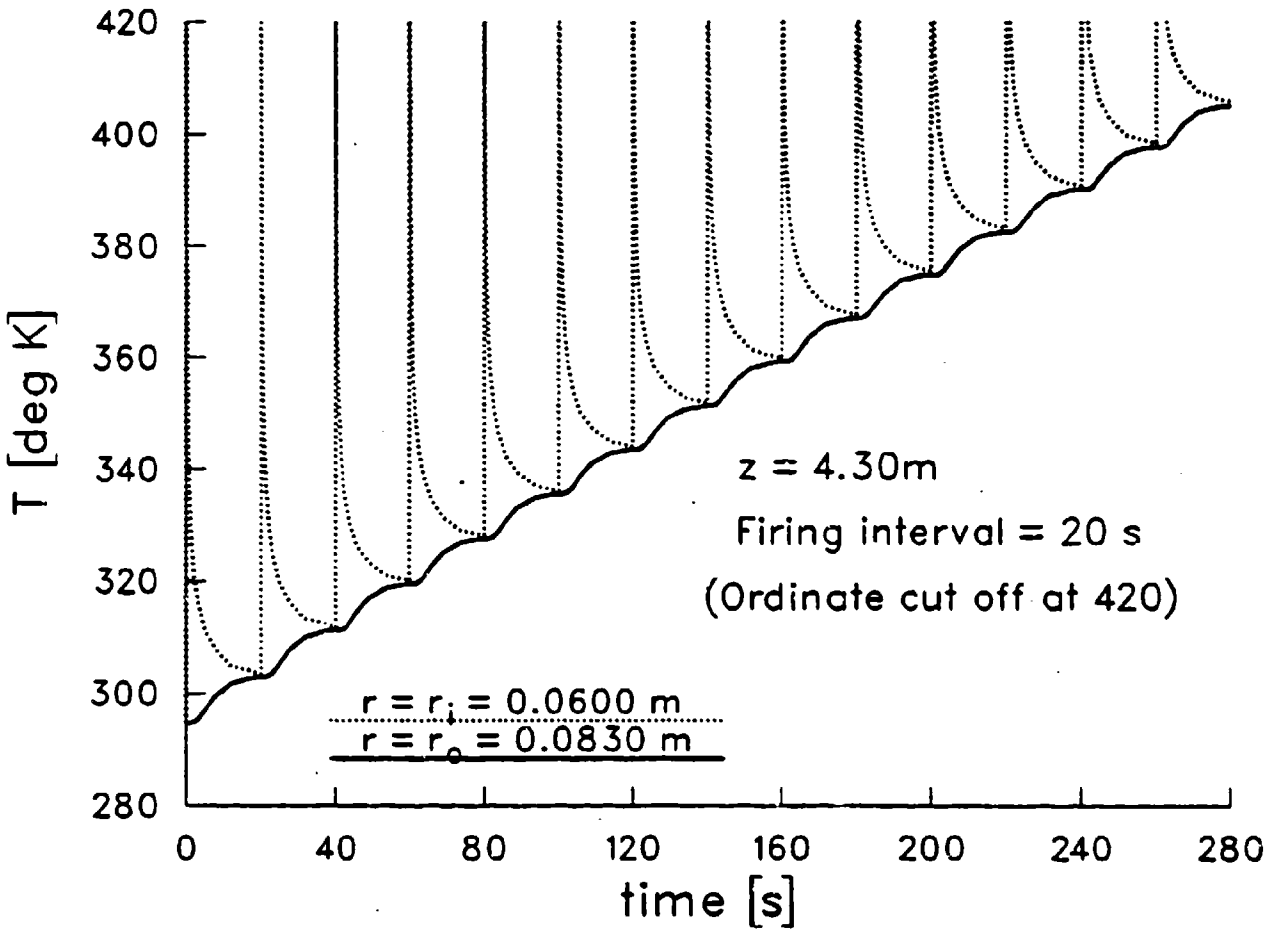

Figure 10. Fast Rate-of-Fire: Inner and Outer Wall Temperature Histories.

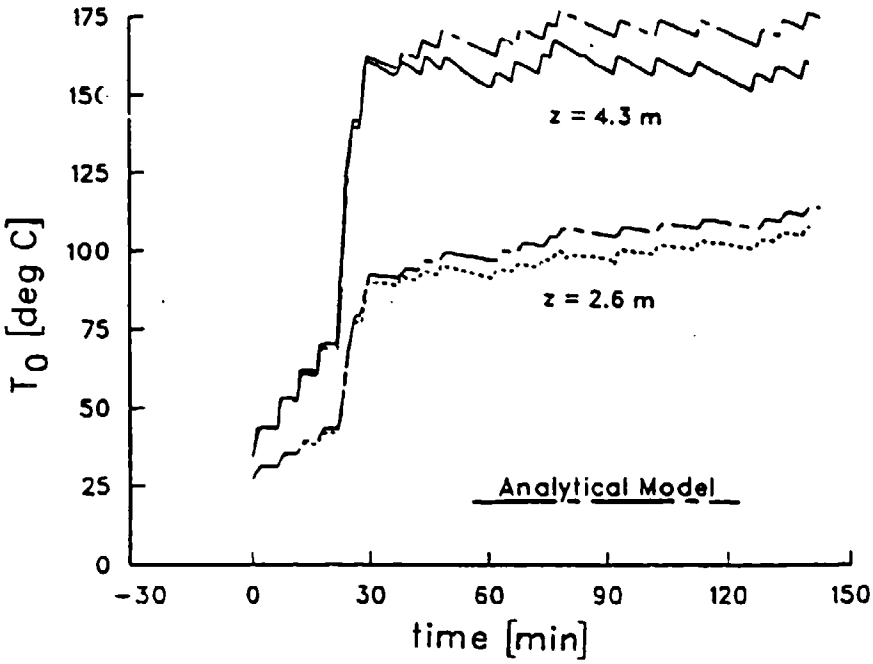

Figure 11. Outer Wall Temperature: Bundy Model and Experimental Results (Sequence of 4 Slow, 14 Rapid, 13 Slow Rounds).

8. DISCUSSION

A limited number of comparisons for a single gun system were made in Section 6 between outputs of the present computer model and experimental data. The resulting favorable agreement indicates that this simulation can yield reasonable predictions of gun tube heating.

It is our intention to remove some of the limitations of the present model. Extension to the two dimensional (radial and axial) unsteady heat conduction problem will undoubtedly be laborious. However, two less difficult, but nonetheless significant, refinements can be made to the one-dimensional model. The first is the addition of a thin layer (0.15 mm) of chrome to the inside wall of the barrel. (This layer is platted onto the gun to decrease erosion.) The second modification is to introduce more accurate input for the physical parameters in the conduction equation and boundary conditions. Thus, for example, c_p and k are actually functions of temperature. This refinement would render the problem analytically non-linear.

It is expected that future interior ballistic input will be produced by an updated version (XKTC) of the NOVA code. This new version will be more "robust" than the present one, and will carry the blowdown calculation further out in time.

9. REFERENCES

Artus, E., and R. Hasenbein. "Thermal Study of the 120-MM M256 Cannon Tube." ARCCB-TR-89028, U.S. Army Armament Research, Development and Engineering Center, Close Combat Armaments Center, Benet Laboratories, Watervliet, NY, October 1989.

Brosseau, T. L., I. C. Stobie, J. R. Ward, and R. W. Geene. "120-mm Gun Heat Input Measurements." BRL-TR-02413, U.S. Army Ballistic Research Laboratory, Aberdeen Proving Ground, MD, July 1982. (AD A118378)

Bundy, M. L. "M256 120-MM Gun Barrel Temperature Model." U.S. Army Ballistic Research Laboratory, Aberdeen Proving Ground, MD, to be published.

Chandra, S., and E. B. Fisher. "Simulation of Barrel Heat Transfer." Final Report, Contract DAAA15-88-D-0014, U.S. Army Ballistic Research Laboratory, Aberdeen Proving Ground, MD, June 1989a.

Chandra, S., and E. B. Fisher. "Analysis of 16-inch/50 Gun Chamber Heating." Veritay Report No. C68-1, Naval Ordnance Station, Indian Head, MD, October 1989b.

Corner, J. Theory of Interior Ballistics of Guns. New York: Wiley, 1950.

Engineering Design Handbook, Ballistic Series. Interior Ballistics of Guns. Chapter 3, AMCP 706-150, U.S. Army Materiel Command, February 1965.

Gough, P. S. "The NOVA Code: A User's Manual - Volume I. Description and Use." IHCR-80-8, Naval Ordnance Station, Indian Head, MD, December 1980.

Heiney, O. K. "Ballistics Applied to Rapid-Fire Guns." Interior Ballistics of Guns, H. Krier and M. Summerfield (eds), vol. 66, Progress in Aeronautics and Astronautics, American Institute of Aeronautics and Astronautics, 1979.

Özisik, M. N. Boundary Value Problems of Heat Conduction. New York: Dover Publications, Inc., 1968.

Rapp, J. R. "Gun Tube Temperature Prediction Model." BRL-MR-3844, U.S. Army Ballistic Research Laboratory, Aberdeen Proving Ground, MD, July 1990. (AD B145792)

Stratford, B. S., and G. S. Beavers. "The Calculation of the Compressible Turbulent Boundary Layer in Arbitrary Pressure Gradient – A Correlation of Certain Previous Methods." Aeronautical Research Council R&M, No. 3207, 1961.

Talley, J. Q. "Barrel Heating and Erosion in the 105mm M68A1E3 Gun Tube." Technical Report, Contract DAAA21-86-C-0350 Amendment P00001, U.S. Army Armament Research, Development and Engineering Center, Picatinny Arsenal, NJ, March 1989a.

Talley, J. Q. "Barrel Heating and Chrome Plate Adhesion in the 120mm M256 Gun Tube." Final Report, Contract DAAA21-85-C-0389, U.S. Army Armament Research, Development, and Engineering Center, Picatinny Arsenal, NJ, September 1989b.

INTENTIONALLY LEFT BLANK.

APPENDIX A:

FORMULAS AND CONSTANTS

INTENTIONALLY LEFT BLANK.

1. From Equation (7), $\zeta = \gamma \xi + (1 - \gamma) \xi^{\beta}$. Then

$$d \zeta / d\xi = \zeta' = \gamma + \beta (1 - \gamma) \xi^{\beta-1}$$

$$d^2 \zeta / d\xi^2 = \zeta'' = \beta (\beta - 1) (1 - \gamma) \xi^{\beta-2} \tag{A.1}$$

2. The functions $g_1(\xi)$, $g_2(\xi)$, and $g_3(\xi)$ occurring in Equation (17) are evaluated by the following sequence:

$$f_1 = 1/(\zeta')^2$$

$$f_2 = (D/\zeta')/(D\zeta + r_i) - \zeta''/(\zeta')^2$$

$$g_1 = (a/D^2)[f_1/(\Delta \xi)^2 - f_2/(2 \Delta \xi)]$$

$$g_2 = -(2 a/D^2) f_1/(\Delta \xi)^2$$

$$g_3 = (a/D^2) [f_1/(\Delta \xi)^2 + f_2/(2 \Delta \xi)]. \tag{A.2}$$

3. The coefficients A_{jn} and d_j in Equation (18) are now given:

For $j = 1$,

$$A_{11} = 3 + 2 \Delta \xi \, D\zeta' (\xi = 0) \, h_g/k$$

$$A_{12} = -4, \qquad A_{13} = 1. \tag{A.3}$$

For $j = NI+1$,

$$A_{NI+1,NI-1} = 1/(2 \Delta \xi), \quad A_{NI+1,NI} = -2/\Delta \xi$$

$$A_{NI+1,NI+1} = 3/(2 \Delta \xi) + h_{\infty} D \zeta' (\xi = 1)/k. \tag{A.4}$$

For $2 \le j \le NI$,

$$A_{j,j-1} = -(\Delta t/2) h_1(\xi_j) \qquad \xi_j = (j-1)\,\Delta\xi$$

$$A_{j,j} = 1 - (\Delta t/2)\, h_2(\xi_j)$$

$$A_{j,j+1} = -(\Delta t/2)\, h_3(\xi_j). \tag{A.5}$$

All other coefficients A_{jk} are equal to zero.

$$d_1 = 2\,\Delta\xi\, D\,\zeta'(\xi = 0)\, h_0\, T_0/k$$

$$d_{NI+1} = h_\infty\, T_\infty\, D\,\zeta'(\xi = 1)/k. \tag{A.6}$$

For $2 \le j \le NI$

$$d_j = T_j^t + (\Delta t/2) G_j^t, \quad \text{where}$$

$$G_j^t = h_1(\xi_j)\, T_{j-1}^t + h_2(\xi_j)\, T_j^t + h_3(\xi_j)\, T_{j+1}^t. \tag{A.7}$$

APPENDIX B:

TIMESCALE SUBROUTINE

INTENTIONALLY LEFT BLANK.

Here, time = t' will refer to time within one firing cycle; $t' = 0$ at the b ginning of the cycle. Six constants are given: t_d, t_f, t_1', t_2', $\Delta t_1'$, and $\Delta t_2'$. Here t_d is the delay time for the rapid rise in T_g and h_g from initial conditions, and t_f is the time between successive firings. The time increment Δt (t') is given by the following function:

$$\Delta t = t_d \qquad 0 \le t' < t_d$$

$$\Delta t = \Delta t_1' \qquad t_d \le t' < t_1'$$

where

$$\Delta t = C_1 + C_2 t' \qquad t_1' \le t' < t_2'$$

$$\Delta t = \Delta t_2' \qquad t_2' \le t',$$

$$C_2 = (\Delta t_2' - \Delta t_1')/(t_2' - t_1') \text{ and } C_1 = \Delta t_2' - C_2\, t_2'$$

$$(\text{If } t' + \Delta t_2' > t_f, \text{ set } \Delta t = t_f - t').$$

A typical set of values of the parameters would be the following:

$$t_1' = 0.018\ s, \quad t_2' = 10.0\ s, \quad \Delta t_1' = 0.00025\ s, \quad \Delta t_2' = 6.0\ s.$$

INTENTIONALLY LEFT BLANK.

APPENDIX C:

OUTLINE OF THERMAL LAYER METHOD

INTENTIONALLY LEFT BLANK.

This method (Özisik 1968) assumes that at early time all the heat transferred from the bore to the barrel lies in a thin layer, of thickness $\delta(t)$, adjacent of the inner wall. For practical purposes, we can apply the conditions

$$T = 0, \quad \partial T/\partial r = 0 \quad \text{at } r = r_i + \partial(t). \tag{C.1}$$

Assume the following approximate form for temperature variation:

$$T = b(t)\,[r - (r_i + \delta)]^2 \ln [r/(r_i + \delta)]. \tag{C.2}$$

This form automatically satisfies the conditions of Equation (C.1). By applying Equation (4) to Equation (C.2), we obtain

$$b = h_{gc}\, T_{gc} / \left\{ (2k\delta + h_{gc}\,\delta^2) \ln [r_i/(r_i + \delta)] - k\,\delta^2/r_i \right\}, \tag{C.3}$$

where h_{gc} and T_{gc} are chosen constants in Equation (22).

Finally, we apply the heat-balance relation obtained by multiplying both sides of Equation (2) by r, integrating from $r = r_i$ to $r = r_i + \delta(t)$, and applying Equation (C.1):

$$-\,[r\,\partial T/\partial r]_{r_i} = (1/\alpha)\,(d/dt) \left[\int_{r_i}^{r_i+\delta(t)} r\,T\,dr \right]. \tag{C.4}$$

This leads to a differential equation of the form $d\delta/dt = f(\delta)$. After some labor, a solution is obtained in $t = t\,(\delta)$ form given by the following sequence of formulas:

$$\varepsilon = \delta/r_i \tag{C.5a}$$

$$\sigma = k/(r_i\,h_{gc}) \tag{C.5b}$$

$$\bar{t} = \alpha\, t/r_i^2 \tag{C.5c}$$

$$c_1 = 3 - 6\sigma \tag{C.5d}$$

$$c_2 = 9\sigma \tag{C.5e}$$

$$\lambda = \frac{3}{2}\sigma \frac{c_2}{c_1^2} \ln c_2 + \left(\frac{1}{4} - \frac{23}{20}\sigma\right) \frac{c_2^2}{c_1^3} \left(\frac{3}{2} - \ln c_2\right) \tag{C.5f}$$

$$B(\varepsilon) = c_1\, \varepsilon + c_2 \tag{C.5g}$$

$$\bar{t} \equiv \left(\frac{1}{4} - \frac{23}{20}\sigma\right) \frac{1}{c_1^3} \left[\frac{1}{2} B^2 - 2\, c_2\, B + c_2^2 \ln B\right] + \lambda$$

$$+ \frac{3}{2}\sigma \left[\frac{\varepsilon}{c_1} + \frac{c_2}{c_1^2} \ln B\right].$$

In the above derivation, several approximations were made via series expansions on the assumption that $\varepsilon << 1$.

LIST OF SYMBOLS

A_{jn}	coefficient in linear equations for barrel temperature, Equation (18)
c_p	specific heat of gun barrel [joules/kg K)]
D	$= r_o - r_i$ [m, mm], thickness of gun barrel
d_j	coefficient in linear equations for barrel temperature, right hand side of Equation (18)
f_1, f_2	given functions of ξ, Equation (3)
$G(\xi,t)$	function for ξ and t defined in Equation (8)
g_1, g_2, g_3	functions of ξ in Equation (17), defined in Appendix A
h_g	heat transfer coefficient - bore gas to gun barrel [joules/(m^{2}s K)]
h_∞	heat transfer coefficient - gun barrel to ambient air [joules/(m^{2}s K)]
j	index indicating radial location of a nodal point in finite difference calculation
k	thermal conductivity of gun barrel [joules/(m s K]
ℓ	index indicating time at which temperature is calculated
NI	number of intervals in $r_i \le r \le r_o$ formed by the nodal points
NR	number of rounds fired
Q_A	$= Q_b/(2\pi r_i)$
Q_b	increase in quantity of heat in gun barrel since $t = 0$, per unit length of barrel [joules/m]
Q_g, Q_∞	quantities of heat per unit length of barrel that have entered the gun barrel through inner and outer walls, respectively, since t = 0 [joules/m]
Q_t	$= Q_g + Q_\infty$
r	radial coordinate in transverse plane [m, mm] ($r = 0$ at axis of gun bore)
r_i, r_o	radial coordinate of inner and outer walls, respectively, of gun barrel [*m, mm*]
T	temperature in the barrel [K]

T_g, T_∞	temperatures in the bore and ambient air, respectively, [K]
T_i, T_o	temperatures at inner and outer walls, respectively, of gun barrel [K]
T_j	$= T(\xi = [j-1]\Delta\xi)$
t	time from initiation of first round [*s, ms, min*]
t_B	matching time for T_g and h_g extrapolation (Section 3) [*s*]
t_d	delay time at given z for rapid rise in T_g and h_g [*s, ms*]
t_f	time between two successive firings [*s, ms*]
t_r	rise time [*s, ms*]
t'	time measured within a firing cycle [*s, ms*]
t_1', t_2'	two prescribed time values in Timescale subroutine, Appendix B [*s*]
y	$= r - r_i$ = penetration depth in barrel [m, mm]
z	axial coordinate ($z = 0$ at breech) [m]
α	$= k/(\rho\, c_p)$ thermal diffusivity of gun barrel [m^2/s] Equation (2)
β, γ	prescribed constants in transformation formula, Equation (7)
$\delta(t)$	thickness of thermal layer in approximate method, Appendix C
Δr	radial distance between two adjacent nodal points [m]
$\Delta t(t)$	time increment for calculation of temperature profile (Equation 15) [*s*]
$\Delta t_1', \Delta t_2'$	two prescribed time increments in the Timescale subroutine, Appendix B [*s*]
$\Delta\xi$	constant increment in ξ in range $0 \le \xi \le 1$; $\Delta\xi = 1/N$
ζ	transformation variable, given in Equation (7)
θ	azimuthal coordinate in transverse plane
ξ	transformed variable, Equation (7); independent variable in transformed Fourier equation, Equation (8)
ρ	density of gun barrel metal [kg/m^3]

No. of Copies	Organization
2	Administrator Defense Technical Info Center ATTN: DTIC-DDA Cameron Station Alexandria, VA 22304-6145
1	Commander U.S. Army Materiel Command ATTN: AMCDRA-ST 5001 Eisenhower Avenue Alexandria, VA 22333-0001
1	Commander U.S. Army Laboratory Command ATTN: AMSLC-DL 2800 Powder Mill Road Adelphi, MD 20783-1145
2	Commander U.S. Army Armament Research, Development, and Engineering Center ATTN: SMCAR-IMI-I Picatinny Arsenal, NJ 07806-5000
2	Commander U.S. Army Armament Research, Development, and Engineering Center ATTN: SMCAR-TDC Picatinny Arsenal, NJ 07806-5000
1	Director Benet Weapons Laboratory U.S. Army Armament Research, Development, and Engineering Center ATTN: SMCAR-CCB-TL Watervliet, NY 12189-4050
(Unclass. only)1	Commander U.S. Army Armament, Munitions and Chemical Command ATTN: AMSMC-IMF-L Rock Island, IL 61299-5000
1	Director U.S. Army Aviation Research and Technology Activity ATTN: SAVRT-R (Library) M/S 219-3 Ames Research Center Moffett Field, CA 94035-1000

No. of Copies	Organization
1	Commander U.S. Army Missile Command ATTN: AMSMI-RD-CS-R (DOC) Redstone Arsenal, AL 35898-5010
1	Commander U.S. Army Tank-Automotive Command ATTN: ASQNC-TAC-DIT (Technical Information Center) Warren, MI 48397-5000
1	Director U.S. Army TRADOC Analysis Command ATTN: ATRC-WSR White Sands Missile Range, NM 88002-5502
1	Commandant U.S. Army Field Artillery School ATTN: ATSF-CSI Ft. Sill, OK 73503-5000
(Class. only)1	Commandant U.S. Army Infantry School ATTN: ATSH-CD (Security Mgr.) Fort Benning, GA 31905-5660
(Unclass. only)1	Commandant U.S. Army Infantry School ATTN: ATSH-CD-CSO-OR Fort Benning, GA 31905-5660
1	Air Force Armament Laboratory ATTN: WL/MNOI Eglin AFB, FL 32542-5000
	Aberdeen Proving Ground
2	Dir, USAMSAA ATTN: AMXSY-D AMXSY-MP, H. Cohen
1	Cdr, USATECOM ATTN: AMSTE-TC
3	Cdr, CRDEC, AMCCOM ATTN: SMCCR-RSP-A SMCCR-MU SMCCR-MSI
1	Dir, VLAMO ATTN: AMSLC-VL-D
10	Dir, BRL ATTN: SLCBR-DD-T

No. of Copies	Organization
12	Director Benet Weapons Laboratory US Army Armament Research, Development, and Engineering Center ATTN: T. Allen P. O'Hara B. Artus SMCAR-CCB-DS, R. Hasenbein SMCAR-CCB-DA, J. Neice J. Cox G. Carafano SMCAR-CCB-DS, P. Votis SMCAR-CCB-DS, C. Andrade SMCAR-LEP-D, J. Zweig SMCAR-CCB, L. Johnson SMCAR-CCB-DA, L. Bennett Watervliet, NY 12189-4050
1	Commander US Army Tank-Automotive Command ATTN: SFAE-ASM-AB-SW, Dr. Pattison Warren, MI 48397-5000
6	Commander Tank Main Armament System ATTN: SFAE-AR-TMA, K. Russel E. Kopacz K. Russell K. Ruben F. Hildebrand S. Bernstein Picatinny Arsenal, NJ 07806-5000
2	Commander US Army Armament, Research, Development, and Engineering Center ATTN: SMCAR-CCH, E. Del Coco K. Pfleger Picatinny Arsenal, NJ 07806-5000
1	President US Army Armor and Engineering Board ATTN: ATSB-WP-ORSA, A. Pomey Fort Knox, KY 40121

No. of Copies	Organization
1	Paul Gough Associates, Inc. ATTN: Dr. Paul S. Gough 1048 South St. Portsmouth, NH 03801-5423
3	Veritay Technology Incorporated ATTN: S. Chandra E. B. Fisher J. Z. Talley P.O. Box 305 4845 Millersport Highway East Amhurst, NY 14051

USER EVALUATION SHEET/CHANGE OF ADDRESS

This laboratory undertakes a continuing effort to improve the quality of the reports it publishes. Your comments/answers below will aid us in our efforts.

1. Does this report satisfy a need? (Comment on purpose, related project, or other area of interest for which the report will be used.) _____

2. How, specifically, is the report being used? (Information source, design data, procedure, source of ideas, etc.) _____

3. Has the information in this report led to any quantitative savings as far as man-hours or dollars saved, operating costs avoided, or efficiencies achieved, etc? If so, please elaborate. _____

4. General Comments. What do you think should be changed to improve future reports? (Indicate changes to organization, technical content, format, etc.) _____

BRL Report Number BRL-MR-3932 Division Symbol _____

Check here if desire to be removed from distribution list. ____

Check here for address change. ____

Current address: Organization _____
Address _____

DEPARTMENT OF THE ARMY
Director
U.S. Army Ballistic Research Laboratory
ATTN: SLCBR-DD-T
Aberdeen Proving Ground, MD 21005-5066

OFFICIAL BUSINESS

BUSINESS REPLY MAIL
FIRST CLASS PERMIT No 0001, APG, MD

Postage will be paid by addressee.

NO POSTAGE NECESSARY IF MAILED IN THE UNITED STATES

Director
U.S. Army Ballistic Research Laboratory
ATTN: SLCBR-DD-T
Aberdeen Proving Ground, MD 21005-5066